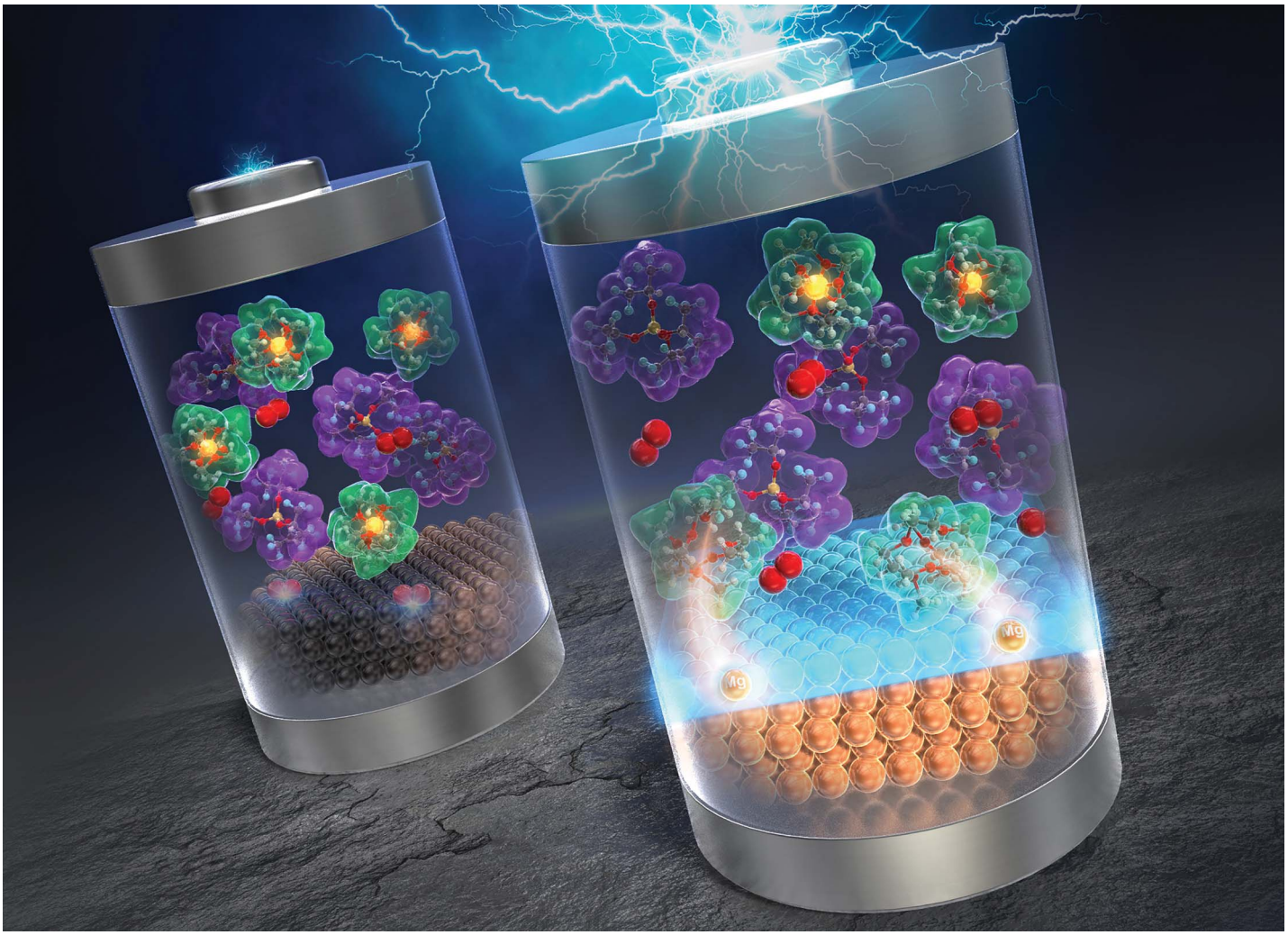

Showcasing research from Dr. Toshihiko Mandai's group, Center for Green Research on Energy and Environmental Materials, National Institute for Materials Science (NIMS), Japan.

Oxygen – a fatal impurity for reversible magnesium deposition/dissolution

Systematic research revealed that O_2, even in miniscule amounts, in the electrolyte solution is a fatal impurity for the reversible electrochemistry of magnesium metals. Complex interfacial processes induced by O_2, magnesium, and electrolyte make firm insulating layer on the surface. The authors also demonstrated the feasibility of constructing an alloy barrier layer on the surface of magnesium to improve its air stability.

As featured in:

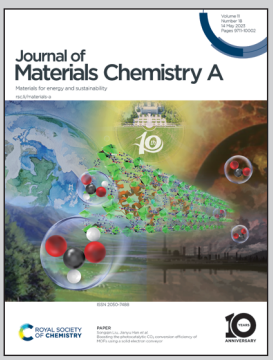

See Toshihiko Mandai and Mariko Watanabe,
J. Mater. Chem. A, 2023, **11**, 9755.

ROYAL SOCIETY OF CHEMISTRY

rsc.li/materials-a

Registered charity number: 207890

Journal of Materials Chemistry A

ROYAL SOCIETY OF CHEMISTRY

COMMUNICATION

View Article Online
View Journal | View Issue

Cite this: J. Mater. Chem. A, 2023, 11, 9755

Received 2nd March 2023
Accepted 9th April 2023

DOI: 10.1039/d3ta01286g

rsc.li/materials-a

Oxygen – a fatal impurity for reversible magnesium deposition/dissolution†

Toshihiko Mandai *[ab] and Mariko Watanabe[a]

The compatibility of rechargeable magnesium batteries (RMBs) with atmospheric components (except moisture) has not been studied. We investigated the effects of atmospheric conditions on the electrochemical dissolution–deposition behavior of magnesium in non-aqueous electrolytes. Oxygen, even in miniscule amounts in the electrolyte was a fatal impurity for reversible magnesium electrochemistry.

Lithium-ion battery (LIB) technology has revolutionized social and industrial structures. To enhance our living environment worldwide while maintaining symbiosis with nature, the performance of energy storage technology must be improved. Among several potential candidate technologies, rechargeable batteries based on magnesium metal negative electrodes are promising due to the geometrical, economical, physicochemical, and electrochemical advantages of the metal. Theoretical energy densities of rechargeable magnesium batteries (RMBs) can reach values that are twice those of present LIBs by combining two-electron electrochemistry at positive electrodes and high volumetric/specific capacities and sufficiently low electrode potential of magnesium at negative electrodes. To realize such outperforming RMBs, research has been conducted on fundamental battery components as well as technologies for interfacial engineering, and a variety of promising materials and techniques have been developed.[1–4] Understanding the fundamental characteristics of battery components is also essential for large-scale battery production and manufacturing.

Every battery component including electrode active materials and electrolytes should be handled under a dry-air atmosphere during the mass production of batteries. Commercialized LIBs are assembled in a dry room with a dew point of −40 °C. From the industrial point of view, the same system should be adoptable for the manufacturing of post-LIBs. To determine their potentials for RMB fabrication, the intrinsic electrochemical characteristics of electrodes and conductive electrolytes under a dry-air atmosphere must be known.

Magnesium deposition/dissolution is the fundamental electrochemical reaction of the negative electrode of RMBs. It is well known in the RMB research field that the reaction activity of magnesium negative electrodes is sensitive to the water content of ethereal solutions.[5] Simple salt-solvent solutions of magnesium bis(trifluoromethanesulfonyl)amide ($Mg[TFSA]_2$) and magnesium tetrakis(hexafluoroisopropoxyl)borate ($Mg[B(HFIP)_4]_2$), which have a relatively high water content (>50 ppm), are reported not to support reversible magnesium deposition/dissolution at negative electrodes, whereas it is known that a small amount of water enhances the interfacial and bulk kinetics at positive electrodes.[6] Water impurities facilitate magnesium passivation associated with $[TFSA]^-$ decomposition,[7] leading to an electrochemically retarded magnesium negative electrode. $Mg[Al(HFIP)_4]_2$-based electrolytes are rather insensitive to water impurities because these electrolytes allow reversible deposition/dissolution, even at high concentrations of impurities (up to 1000 ppm).[8] In contrast to these extensive studies on the water impurities in RMB electrolytes, the compatibility of RMB components with dry air, especially O_2 gas, remains unclear. This might be due to the uncertain preconception and misunderstanding of the passivation characteristics of magnesium, namely, that a magnesium metal can be easily oxidized to form insulative oxide on the surface upon exposure to an ambient air atmosphere.[9] To understand the intrinsic electrochemistry of magnesium metal negative electrodes, reversible magnesium deposition/dissolution were analyzed under different atmospheric conditions in this study. The results of combined electrochemical

[a]Center for Green Research on Energy and Environmental Materials, National Institute for Materials Science (NIMS), 1-1 Namiki, Tsukuba, Ibaraki, 305-0044, Japan. E-mail: mandai.toshihiko@nims.go.jp; Tel: +81-29-860-4464

[b]Center for Advanced Battery Collaboration, Center for Green Research on Energy and Environmental Materials, National Institute for Materials Science (NIMS), 1-1 Namiki, Tsukuba, Ibaraki, 305-0044, Japan

† Electronic supplementary information (ESI) available: Experimental detail and supporting figures and tables are provided. See DOI: https://doi.org/10.1039/d3ta01286g

and spectroscopic investigations reveal that O_2 is a fatal impurity in RMB (electro)chemistry. In addition, an effective surface treatment to sustain sufficient electrochemical activities, even under an O_2 atmosphere, is provided.

The compatibility of RMB components, especially magnesium metal negative electrodes and electrolytes incorporating representative air-stable weakly-coordinated anions $[B(HFIP)_4]^-$ or $[Al(HFIP)_4]^-$ with dry air was investigated. The results of a simple experimental survey demonstrated the sensitivity of magnesium metals to O_2, due to reversible magnesium deposition/dissolution being possible when using magnesium metals polished under dry air, where the dew point was controlled at approximately −70 °C (Fig. S1†). The Mg 2p and O 1s spectra and depth profiles of magnesium metals indicate the presence of an oxide- and carbonate-based layer, the so-called native solid electrolyte interface (SEI), on the outermost surface, independent of the polishing environment (Fig. S2 and S3†). This suggests that the native SEI does not necessarily impede electrochemical magnesium deposition/dissolution reactions. However, cells assembled under a dry-air atmosphere show no features of electrochemical magnesium deposition/dissolution (Fig. S1†).

To identify what factor has a significant detrimental effect on the electrochemical characteristics of magnesium metal negative electrodes and electrolytes, systematic cyclic voltammetry (CV) and open-circuit potential (OCP) measurements were conducted under certain atmospheric conditions with Ar, N_2, and O_2 and an air-tight voltammetry cell equipped with gas-inlet lines. After 30 min of steady flow of each gas at 10 mL min^{-1} in the voltammetry cell (volume of ~30 mL) assembled in an Ar-filled glovebox, the Pt and Mg working electrodes showed characteristic responses dependent on the inlet gases (Fig. 1). Similar to Ar gas, N_2 gas also has minor or rather favorable effect on the electrochemical magnesium deposition/dissolution activity. In contrast, O_2 gas is detrimental to the electrochemical activities, independent of the working electrodes. The time-profile of OCP during the steady flow of different gases supports the change in the nature of the magnesium electrodes, especially under an O_2 atmosphere (Fig. 1c). The electrode potential of magnesium metal increased by ~200 mV after 30 min of steady flow of O_2, accompanied by the continuous increase of the O_2 concentration in the electrolytes. CV measurements were conducted immediately after 1 and 5 min of steady flow of an O_2 gas at the same rate. The results show that the introduction of O_2 gas is fatal for reversible magnesium deposition/dissolution (Fig. S4†), because O_2 in the electrolyte solution, even at 17 ppm, inactivates the magnesium negative electrodes. Fig. S4b† shows that the inactivation of the magnesium electrodes by O_2 is a dynamic process. The introduction of O_2 in the electrolyte solution and resulting insulative layer formation on magnesium electrodes seem to be irreversible and catastrophic, because subsequent Ar bubbling to deoxygenate the electrolytes did not recover the electrochemical activities (Fig. S5†). The control measurements using the deoxygenated electrolyte and fresh magnesium pieces showed reversible magnesium deposition/dissolution activity (Fig. S6†). It should be noted here that the introduction of O_2 can affect the water content of the electrolytes, possibly owing to our experimental setup. However, the detrimental effect of water impurity seems negligible as the electrolytes containing

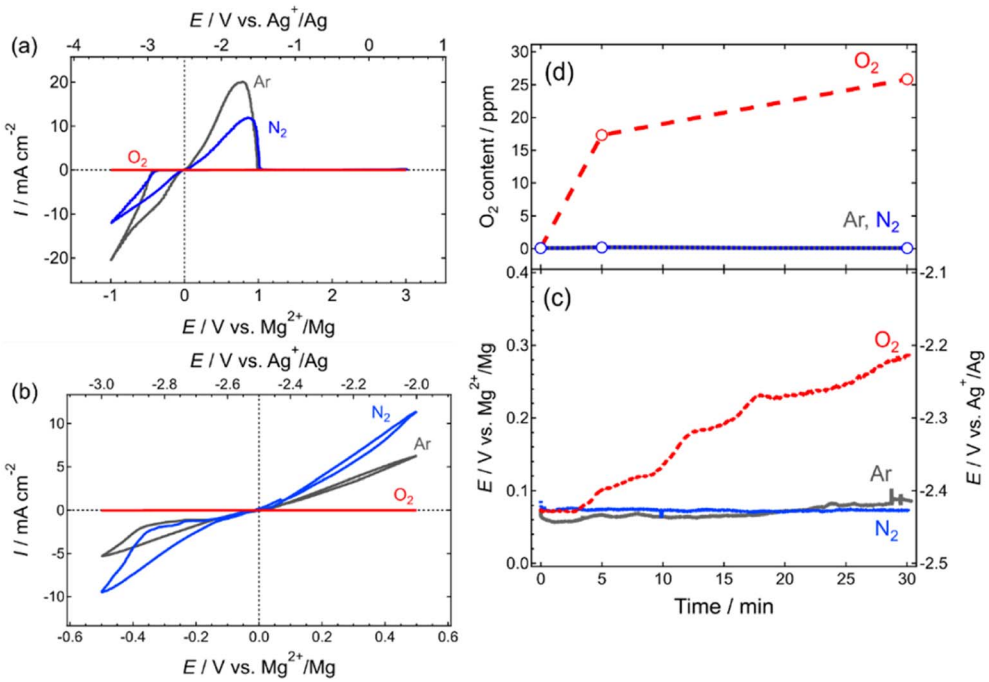

Fig. 1 CV and OCP profiles of Pt and Mg electrodes under steady flow of different gases recorded in 0.3 mol dm^{-3} $Mg[B(HFIP)_4]_2$/G2 electrolytes. CV profiles using (a) Pt and (b) Mg working electrodes. Time profiles of (c) OCV of Mg electrodes and (d) corresponding O_2 concentration in electrolyte solutions. The time profiles of O_2 concentrations under N_2 and Ar were zero during measurements.

>100 ppm of water represent favorable magnesium electrochemistry (Fig. S7†). In contrast, the ionic conductivities and Raman spectra of the electrolytes are invariable, even after 30 min of O_2 gas flow (Table S1 and Fig. S8†), implying that the electrolytes are chemically stable against O_2. These results strongly suggest that soaking magnesium metal in an electrolyte with O_2 impurities retards the electrochemical activity of magnesium deposition/dissolution. Note that the potential shift of the reference electrode (Ag^+/Ag) is negligible because the equilibrium potential for the magnesium dissolution process remains unchanged, even after exposure to dry air (see Fig. S4†).

The sensitivity of electrochemical magnesium deposition/dissolution activities to O_2 impurities seems to be electrolyte-independent. Electrolyte solutions of $Mg[TFSA]_2$ did not support electrodeposition of magnesium under a dry-air atmosphere, irrespective of the presence/absence of Cl-based activation reagents (Fig. S9†), although the electrolyte components themselves are chemically stable against air and moisture.[10]

X-ray photoelectron spectroscopy (XPS) and electrochemical impedance spectroscopy (EIS) provide further insights into the surface chemical states of magnesium metals soaked in an electrolyte with and without O_2 impurities. Fig. 2 shows the Mg 2p, F 1s, and O 1s spectra of certain magnesium strips. All the Mg 2p, F 1s and O 1s spectra of magnesium strips soaked in the electrolyte under an Ar atmosphere have distinct peaks certainly assignable to the products due to the adsorption and/or side reaction of the electrolyte anion with magnesium metal, such as $MgCO_3$, MgF_2, $Mg(OH)_2$, CF_n, and B–O compounds (Fig. 2a–c). These results imply the strong reductive nature of magnesium under an inert atmosphere. In contrast, the F 1s and O 1s spectra of magnesium strips soaked in electrolytes with O_2 impurities exhibit small MgF_2 and negligible B–O compound peaks, suggesting the suppressed adsorption and subsequent decomposition of the anions on the surface. The Mg 2p and O 1s spectra show rather distinct contributions of MgO and $Mg(OH)_2$ on the surface of strips soaked in electrolytes with O_2. The EIS spectra of symmetric [Mg||Mg] cells also demonstrate the detrimental effect of O_2 impurity. The extremely large interfacial resistance was observed for the cells assembled using the electrolytes with O_2 impurity (Fig. 2g). The cells using the electrolyte deoxygenated by Ar bubbling showed a substantially low resistance, again emphasizing that the presence of O_2 impurities in the electrolytes significantly affects the electrochemical magnesium deposition/dissolution activity. The oxide- and hydroxide-based highly-insulative layer generated at the magnesium–electrolyte–O_2 three-phase boundary may represent a factor affecting the reversible electrochemistry (Fig. 2h and i).

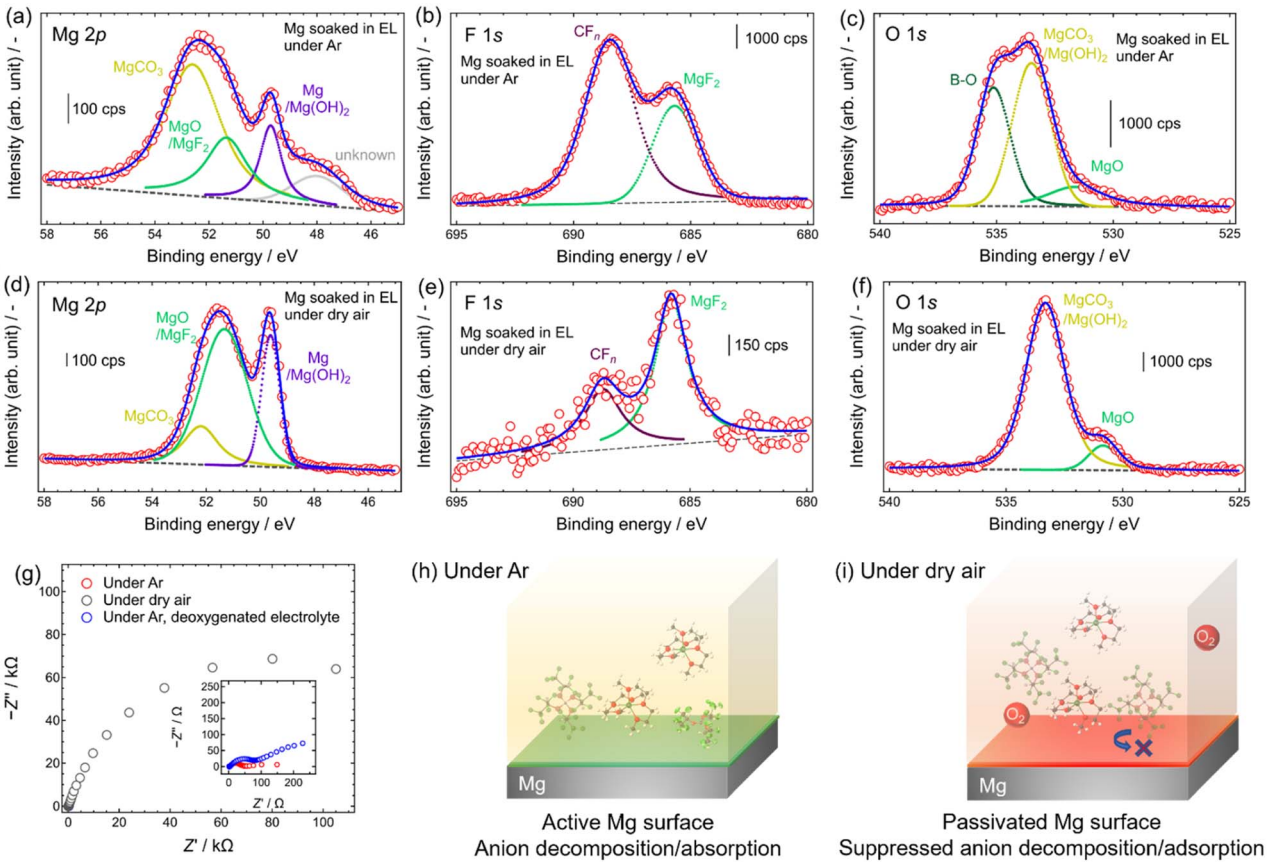

Fig. 2 Surface Mg 2p, F 1s, and O 1s spectra of Mg strips soaked in electrolyte solutions under (a–c) Ar and (d–f) dry-air atmospheres. (g) EIS spectra of symmetric [Mg||Mg] cells. Schematic illustrations of the surface chemistry of magnesium electrodes under (h) Ar and (i) dry-air atmosphere.

The above-mentioned characteristics of magnesium metals will limit the mass production of RMBs. Therefore, techniques to overcome such a limitation must be developed. The magnesium electrochemistry under an O_2 atmosphere has been extensively studied in the magnesium–air battery field. Similar to conventional aqueous zinc–air batteries, reactions at the magnesium negative electrode side in alkaline media could lead to the corrosion of the magnesium metal and magnesium hydroxide formation upon discharge.[11] However, due to the large overpotential, reverse reactions do not proceed. Thus, most aqueous magnesium–air batteries are primary and not secondary batteries. Non-aqueous magnesium–oxygen batteries have also been reported, and reversible cycling has been achieved with a specific redox mediator, that is, an I_2-DMSO complex, in the $Mg(ClO_4)_2$-dimethylsulfoxide electrolyte.[12] The above-mentioned non-aqueous electrolyte does not support magnesium electrodeposition. The charge–discharge profiles of magnesium–oxygen batteries indicate a poor reversibility, presumably due to the electrochemical inactivity at the magnesium negative electrode side.

The surface functionalization by an artificial interface is an effective approach to modify the chemical nature of the substrate surface. *Ex*/*in situ*-fabricated artificial magnesiophilic interfaces can mitigate undesired side reactions between magnesium negative electrodes and electrolytes and thus enhance the interfacial magnesium deposition/dissolution kinetics.[4] Among various options, $BiCl_3$-based surface functionalization yields a significant charge–discharge reversibility of hybrid magnesium–lithium–oxygen batteries in non-aqueous media.[4] Although the detailed electrochemistry at the modified negative electrodes in that system remains unclear, the results of our study demonstrate reversible magnesium deposition/dissolution on the $BiCl_3$-treated magnesium metal under a dry-air atmosphere (Fig. 3a). As bismuth can form magnesium alloys, that is, Mg_3Bi_2, certain hybrid metal–alloy interfaces may function as a magnesium ion-conductive barrier layer,[4d] which supports reversible electrochemistry, even in the presence of O_2 impurities. To optimize the interfacial chemical composition, screening surveys of alloying elements were conducted by adopting a simple dipping treatment methodology (detailed methods are described in the ESI†). As the chemical reduction of alloying element ions by magnesium metal, known as a galvanic replacement reaction, is a driving force of spontaneous alloying reactions, alloying elements that can be reduced

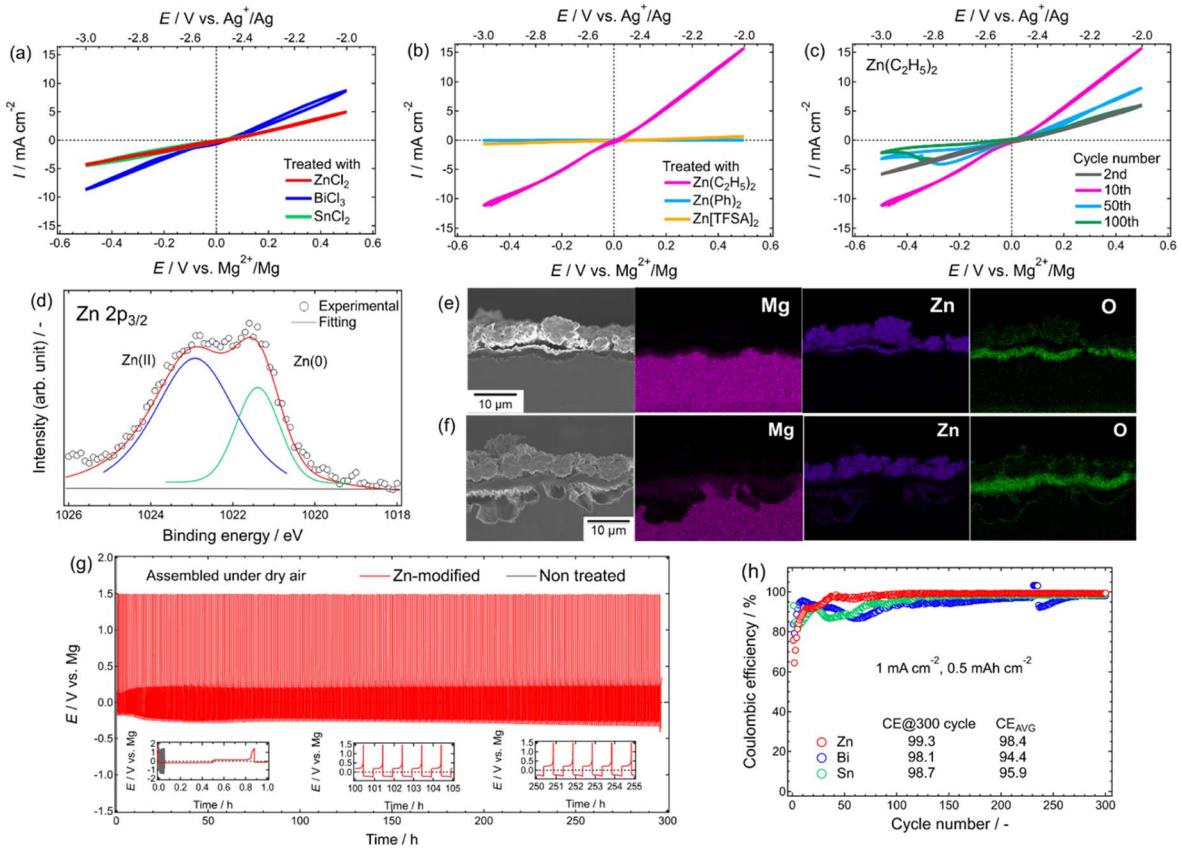

Fig. 3 CV profiles of modified Mg electrodes recorded in 0.3 mol dm^{-3} $Mg[B(HFIP)_4]_2$/G2 electrolytes measured under a dry-air atmosphere. Mg electrodes were modified using ethereal solutions of (a) metal chlorides and (b) zinc-based non-chloride compounds. (c) Prolonged CV profiles of zinc-modified Mg electrodes. (d) Zn $2p_{3/2}$ XPS spectrum of zinc-modified Mg. SEM images and corresponding EDX profiles of cross-sectional views of zinc-modified Mg electrodes after (e) preparation and (f) single dissolution processes. (g) Galvanostatic cycling profiles of [Mg||Cu] cells assembled under a dry-air atmosphere using zinc-modified and untreated Mg electrodes measured at 1 mA cm^{-2} and (h) corresponding coulombic efficiency including the results using bismuth- and tin-modified Mg electrodes.

by magnesium metal should be adoptable. Our results show that magnesium electrodes treated with reductive lithium and calcium-bearing solutions do not support electrochemical magnesium deposition/dissolution reactions (Fig. S10†).

Based on the survey, chloride compounds of elements capable of forming alloys with magnesium will lead to the fabrication of favorable interfaces. Magnesium metals treated with $BiCl_3$, $SnCl_2$, and $ZnCl_2$ solutions facilitate reversible magnesium dissolution/deposition under a dry-air atmosphere (Fig. 3a). Except for zinc-based compounds, treatments using neither compounds of non-alloying elements paired with chloride (*e.g.*, $NiCl_2$) nor organometallic compounds of alloying elements (*e.g.*, $Bi(phenyl)_3$ and $Sn(CH_3)_4$) resulted in inactive interfaces (Fig. S11†). Chloride may solely impart effective interfaces, because magnesium metals treated with a typical Grignard reagent have slightly active CV profiles (Fig. S12†). These results indicate that hybrid interfaces consisting of alloying elements and chlorides may be particularly favorable for reversible magnesium dissolution/deposition under a dry-air atmosphere. XPS and energy-dispersive X-ray spectroscopy (EDX) spectra indicate the formation of such interfaces using simple soaking treatments (Fig. S13 and S14†). Scanning electron microscopy (SEM) images of cycled magnesium electrodes show that such artificial interfaces facilitate electrochemical magnesium dissolution/deposition, because preferential reaction sites are located in the vicinity of alloying compounds (Fig. S15†). Among the aforementioned alloying elements, zinc can impart favorable interfaces despite the absence of chloride species (Fig. 3b). As chloride species can lead to undesired cell failure due to their highly corrosive nature,[13] chloride-free artificial interfaces are preferred in practical battery applications.[5b] Specifically, magnesium metals pretreated with the $Zn(C_2H_5)_2$ solution supported the remarkable electrochemical magnesium dissolution/deposition activity. $Zn(C_2H_5)_2$-modified magnesium retained its favorable electrochemical activity for more than 5 h, even at an equilibrium O_2 concentration under standard atmospheric conditions (Fig. 3c). These outstanding characteristics of zinc-modified interfaces might be due to the O_2 gas barrier properties of Zn/ZnO.[14] Zn $2p_{3/2}$ spectra, SEM images, and corresponding EDX profiles of the cross-sectional view of pristine and cycled zinc-modified magnesium electrodes indicate the formation of a magnesium ion-conductive Zn/ZnO layer upon the chemical reduction of zinc species in pretreatment solutions by magnesium, because magnesium dissolution/deposition was evident thorough that layer (Fig. 3e and f). Closed Swagelok-type cells fabricated under a dry atmosphere facilitate reversible magnesium dissolution/deposition cycling for sufficiently long periods at a current density of 1 mA cm^{-2} (Fig. 3g). However, the reactivity gradually diminishes, possibly due to the inactivation of progressively generated, untreated magnesium surfaces upon the exposure to O_2 gas during CV measurements under open beaker-type cells. The surface modification by zinc seems particularly effective, because relatively stable cycling was achieved with zinc-modified magnesium electrodes compared with bismuth- and tin-modified counterparts (Fig. 3h and S16†). The smaller lattice mismatch between both *hcp* magnesium and zinc metals as well as good compatibility of MgO and ZnO[4e,15] resulted in a well-integrated interface, and are likely the reasons for the stable magnesium dissolution/deposition cycling. Note that the typical magnesium–zinc solid solution is electrochemically inactive under a dry-air atmosphere (Fig. S17†). This infers the specific function of the chemically generated zinc-based interface. Full cells assembled under a dry-air atmosphere were successfully cycled using Mo_6S_8 and α-MnO_2 positive electrodes and zinc-modified magnesium negative electrodes, as shown in Fig. 4, while inferior cycling performances were observed for the cells using non-modified magnesium. These results further corroborate the favorable O_2 barrier characteristics of the zinc-based interface. Recently, a successful cycling of RMB full cells fabricated under a dry-air atmosphere was reported.[16] However, the inferior battery performance of those cells, when compared to the performance of the cells fabricated under an Ar atmosphere, implies a severe detrimental effect of O_2 impurity on reversible magnesium electrochemistry.

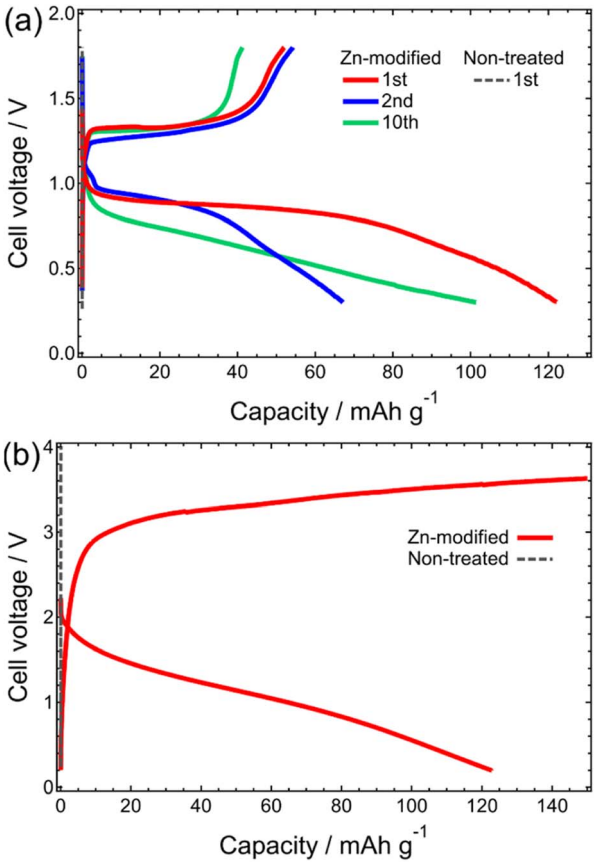

Fig. 4 Discharge–charge profiles of (a) [Zn-modified Mg||Mo_6S_8] and (b) [Zn-modified Mg||α-MnO_2] cells assembled under a dry-air atmosphere. The profiles using non-modified Mg negative electrodes are included as reference profiles.

Conclusions

The systematic study of magnesium negative electrodes under different atmospheric conditions reveals that O_2 in electrolyte

solutions is a fatal impurity for the reversible electrochemistry of magnesium metal. The results of our analyses indicate the insulating/barrier characteristics of the firm oxide- and hydroxide-based interface with respect to magnesium ion conduction, which might be induced by complex O_2, magnesium, and electrolyte (solvent)-related interfacial processes. Appropriate surface modification of magnesium negative electrodes by zinc species can be used to prevent such an undesired situation. Although the formation and magnesium ion transport mechanisms must be further studied and insights into zinc-based interfaces must be provided to maximize those benefits, our results provide guidance for the construction of manufacturing systems for practical RMBs based on the diversion of existing LIB systems.

Author contributions

T. Mandai – data curation, funding acquisition, formal analysis, investigation, project administration, validation, writing of original draft (lead). M. Watanabe – data curation (supporting).

Conflicts of interest

There are no conflicts to declare.

Acknowledgements

The authors thank Ms Makiko Oshida, Mr Keisuke Shinoda, and Mr Kazuo Yamaguchi for their support with SEM and TEM observations and XPS measurements at the Battery Research Platform of National Institute for Materials Science. This work was financially supported by the Advanced Low-Carbon Technology-Specially Promoted Research for Innovative Next Generation Batteries Program (ALCA-SPRING, Grant Number JPMJAL1301), NEXT Center of Innovation Program (COI-NEXT, Grant Number JPMJPF2016) of the Japan Science and Technology Agency, and KAKENHI (Grant No. 21K05263) of the Japan Society for the Promotion of Science.

References

1 (*a*) L. Li, Y. Lu, Q. Zhang, S. Zhao, Z. Hu and S.-L. Chou, *Small*, 2019, **17**, 1902767; (*b*) Z. Zhang, S. Dong, Z. Cui, A. Du, G. Li and G. Cui, *Small Methods*, 2018, **2**, 1800020; (*c*) L. Kong, C. Yan, J.-Q. Huang, M.-Q. Zhao, M.-M. Titirici, R. Xiang and Q. Zhang, *Energy Environ. Mater.*, 2018, **1**, 100–112; (*d*) S. Tan, F. Xiong, J. Wang, Q. An and L. Mai, *Mater. Horiz.*, 2020, **7**, 1971–1995; (*e*) I. D. Johnson, B. J. Ingram and J. Cabana, *ACS Energy Lett.*, 2021, **6**, 1892–1900; (*f*) Z. Yao, Y. Yu, Q. Wu, M. Cui, X. Zhou, J. Liu and C. Li, *Small*, 2021, **17**, 2102168.

2 (*a*) T. S. Arthur, N. Singh and M. Matsui, *Electrochem. Commun.*, 2012, **16**, 103–106; (*b*) A. Maddegalla, A. Mukherjee, J. A. Blázquez, E. Azaceta, O. Leonet, A. R. Mainar, A. Kovalevsky, D. Sharon, J.-F. Martin, D. Sotta, Y. E. Eli, D. Aurbach and M. Noked, *ChemSusChem*, 2021, **14**, 4690–4696; (*c*) T. Mandai and H. Somekawa, *Chem. Commun.*, 2020, **56**, 12122–12125; (*d*) T. Mandai and H. Somekawa, *Batteries Supercaps*, 2022, **5**, e202200153.

3 (*a*) O. Tutusaus, R. Mohtadi, T. S. Arthur, F. Mizuno, E. G. Nelson and Y. V. Sevryugina, *Angew. Chem., Int. Ed.*, 2015, **54**, 7900–7904; (*b*) J. T. Herb, C. A. N. Lund and C. B. Arnold, *ACS Energy Lett.*, 2016, **1**, 1227–1232; (*c*) Z. Z. Karger, M. E. G. Bardaji, O. Fuhr and M. Fichtner, *J. Mater. Chem. A*, 2017, **5**, 10815–10820; (*d*) J. Luo, Y. Bi, L. Zhang, X. Zhang and T. L. Liu, *Angew. Chem., Int. Ed.*, 2019, **58**, 6967–6971; (*e*) T. Mandai, *ACS Appl. Mater. Interfaces*, 2020, **12**, 39135–39144; (*f*) T. Mandai, Y. Youn and Y. Tateyama, *Mater. Adv.*, 2021, **2**, 6283–6296.

4 (*a*) B. Wan, H. Dou, X. Zhao, J. Wang, W. Zhao, M. Guo, Y. Zhang, J. Li, Z.-F. Ma and X. Yang, *ACS Appl. Mater. Interfaces*, 2020, **12**, 28298–28305; (*b*) J. Zhang, X. Guan, R. Lv, D. Wang, P. Liu and J. Luo, *Energy Storage Mater.*, 2020, **26**, 408–413; (*c*) R. Lv, X. Guan, J. Zhang, Y. Xia and J. Luo, *Natl. Sci. Rev.*, 2020, **7**, 333–341; (*d*) Y. Zhao, A. Du, S. Dong, F. Jiang, Z. Guo, X. Ge, X. Qu, X. Zhou and G. Cui, *ACS Energy Lett.*, 2021, **6**, 2594–2601; (*e*) J. Bae, H. Park, X. Guo, X. Zhang, J. H. Warner and G. Yu, *Energy Environ. Sci.*, 2021, **14**, 4391–4399; (*f*) Y. Li, X. Zhou, J. Hu, Y. Zheng, M. Huang, K. Guo and C. Li, *Energy Storage Mater.*, 2022, **46**, 1–9.

5 (*a*) Z. Ma, M. Kar, C. Xiao, M. Forsyth and D. R. MacFarlane, *Electrochem. Commun.*, 2017, **78**, 29–32; (*b*) S. Terada, T. Mandai, S. Suzuki, S. Tsuzuki, K. Watanabe, Y. Kamei, K. Ueno, K. Dokko and M. Watanabe, *J. Phys. Chem. C*, 2016, **120**, 1353–1365; (*c*) S. Yagi, A. Tanaka, Y. Ichikawa, T. Ichitsubo and E. Matsubara, *Res. Chem. Intermed.*, 2014, **40**, 3–9; (*d*) Z. Meng, Z. Li, L. Wang, T. Diemant, D. Bosubabu, Y. Tang, R. Berthelot, Z. Z. Karger and M. Fichtner, *ACS Appl. Mater. Interfaces*, 2021, **13**, 37044–37051.

6 (*a*) G. S. Gautam, P. Canepa, W. D. Richards, R. Malik and G. Ceder, *Nano Lett.*, 2016, **16**, 2426–2431; (*b*) X. Sun, V. Duffort, B. L. Mehdi, N. D. Browning and L. F. Nazar, *Chem. Mater.*, 2016, **28**, 534–542; (*c*) S.-B. Son, T. Gao, S. P. Harvey, K. X. Steirer, A. Stokes, A. Norman, C. Wang, A. Cresce, K. Xu and C. Ban, *Nat. Chem.*, 2018, **10**, 532–539.

7 (*a*) Y. Yu, A. Baskin, C. V. Vidal, N. T. Hahn, Q. Liu, K. R. Zavadil, B. W. Eichhorn, D. Prendergast and E. J. Crumlin, *Chem. Mater.*, 2017, **29**, 8504–8512; (*b*) J. G. Connell, B. Genorio, P. P. Lopes, D. Strmcnik, V. R. Stamenkovic and N. M. Markovic, *Chem. Mater.*, 2016, **28**, 8268–8277.

8 T. Pavčnik, M. Lozinšek, K. Pirnat, A. Vizintin, T. Mandai, D. Aurbach, R. Dominko and J. Bitenc, *ACS Appl. Mater. Interfaces*, 2022, **14**, 26766–26774.

9 H. J. T. Ellingham, *J. Soc. Chem. Ind., London*, 1944, **63**, 125–133.

10 T. Mandai, Y. Akita, S. Yagi, M. Egashira, H. Munakata and K. Kanamura, *J. Mater. Chem. A*, 2017, **5**, 3152–3156.

11 Md. A. Rahman, X. Wang and C. Wenz, *J. Electrochem. Soc.*, 2013, **160**, A1759–A1771.

12 T. Shiga, Y. Hase, Y. Kato, M. Inoue and K. Takechi, *Chem. Commun.*, 2013, **49**, 9152–9154.
13 J. Muldoon, C. B. Bucur, A. G. Oliver, J. Zajicek, G. D. Allred and W. C. Boggess, *Energy Environ. Sci.*, 2013, **6**, 482–487.
14 (*a*) M. Abbas, M. Buntinx, W. Deferme, N. Reddy and R. Peeters, *Nanomaterials*, 2021, **11**, 449; (*b*) V. Chawla, M. Ruoho, M. Weber, A. A. Chaaya, A. A. Taylor, C. Charmette, P. Miele, M. Bechelany, J. Michler and I. Utke, *Nanomaterials*, 2019, **9**, 88.
15 H. Somekawa, *Mater. Trans.*, 2020, **61**, 1–13.
16 (*a*) Y. Xiu, Z. Li, V. B. Parambath, Z. Ding, L. Wang, A. Reupert, M. Fichtner and Z. Z. Karger, *Batteries Supercaps*, 2021, **4**, 1850–1857; (*b*) L. Wang, P. Jankowski, C. Njel, W. Bauer, Z. Li, Z. Meng, B. Dasari, T. Vegge, J. M. G. Lastra, Z. Z. Karger and M. Fichtner, *Adv. Sci.*, 2022, **9**, 2104605.